Eur Biophys J (2011) 40:93–101
DOI 10.1007/s00249-010-0621-z

BIOPHYSICS LETTER

Transiently crosslinked F-actin bundles

Dan Strehle · Jörg Schnauß · Claus Heussinger · José Alvarado · Mark Bathe · Josef Käs · Brian Gentry

Received: 20 April 2010 / Revised: 23 June 2010 / Accepted: 30 July 2010 / Published online: 24 August 2010

Abstract F-actin bundles are prominent cytoskeletal structures in eukaryotes. They provide mechanical stability in stereocilia, microvilli, filopodia, stress fibers and the sperm acrosome. Bundles are typically stabilized by a wide range of specific crosslinking proteins, most of which exhibit off-rates on the order of $1s^{-1}$. Yet F-actin bundles exhibit structural and mechanical integrity on time scales that are orders of magnitude longer. By applying large deformations to reconstituted F-actin bundles using optical tweezers, we provide direct evidence of their differential mechanical response in vitro: bundles exhibit fully reversible, elastic response on short time scales and irreversible, elasto-plastic response on time scales that are long compared to the characteristic crosslink dissociation time. Our measurements show a broad range of characteristic relaxation times for reconstituted F-actin bundles. This can be reconciled by considering that bundle relaxation behavior is also modulated by the number of filaments, crosslinking type and occupation number as well as the consideration of defects due to filament ends.

Keywords Actin bundle mechanics · Transient crosslinkers · Stressfibers · Cytoskeleton · Semiflexible polymers · Optical tweezers

Introduction

The actin cytoskeleton is an essential component of many dynamic cellular processes including wound healing, embryonic development, tissue regeneration, and the immune response (Ridley et al. 2003; Hotulainen and Lappalainen 2006; Howard 2001; Pollard and Earnshaw 2002). As a consequence, the mechanical properties of F-actin networks have been the focus of numerous experimental and theoretical investigations (Janmey et al. 1994; Käs et al. 1996; Heussinger et al. 2007; Koenderink et al. 2009). F-actin bundles, however, have received considerably less attention, despite the fact that cellular F-actin often exists in a crosslinked, bundled state. Indeed, organized bundles of F-actin play important roles in various cell functions, manifesting as filopodia, stress fibers, microvilli, hair cells, the contractile ring, and other cytoskeletal assemblies (Hotulainen and Lappalainen 2006; Bartles 2000; Aratyn et al. 2007; Heintzelman and Mooseker 1992; Roberts et al. 1988). To produce F-actin bundles, cells employ a variety of transiently crosslinking proteins including fascin, fimbrin, and α-actinin (Bartles 2000) which typically bind and unbind on the order of seconds (Xu et al. 1998; Ferrer et al. 2008). The transient connections within a bundle limit its load carrying characteristics.

Electronic supplementary material The online version of this article (doi:10.1007/s00249-010-0621-z) contains supplementary material, which is available to authorized users.

D. Strehle (✉) · J. Schnauß · J. Alvarado · J. Käs · B. Gentry
Soft matter physics division, Institute for Experimental Physics I, University of Leipzig, 04103 Leipzig, Germany
e-mail: dan.strehle@uni-leipzig.de

C. Heussinger
Laboratoire de Physique de la Matière Condensée et Nanostructures, UMR CNRS 5586, Université de Lyon I, 69622 Villeurbanne, France

Present Address:
J. Alvarado · B. Gentry
Biological Soft Matter Group, FOM Institute AMOLF, Science Park 104, 1098 XG Amsterdam, The Netherlands

M. Bathe
Department of Biological Engineering, MIT, 77 Massachusetts Avenue, Cambridge, MA 02139, USA

However, the relaxation rate is not only determined by the binding times of crosslinks but also by factors such as number and type of bound crosslinks and number of filaments per bundle (Bathe et al. 2008). This opens a multitude of relaxation times as they are also found in various mechanical studies (Fabry et al. 2001; Hoffman et al. 2006). Phenomenologically this is strongly reminiscent of the relaxation behavior of soft glasses (Semmrich et al. 2007).

Several in vitro experiments have directly investigated the mechanical properties of filament bundles, illustrating the important role played by bundling proteins (Tolomeo and Holley 1997; Shin et al. 2004; Claessens et al. 2006). One series of experiments performed on thermally fluctuating F-actin bundle rings measured bundle bending stiffness using a variety of crosslink types and concentrations (Claessens et al. 2006). The dependence of bundle stiffness on bundle size and actin-bundling protein type and concentration was systematically elucidated for a broad range of parameters under equilibrium conditions and small bundle deformations induced passively by thermal fluctuations (Claessens et al. 2006; Bathe et al. 2008). In the present study, we focus on large bundle deformations that are actively applied using optical tweezers. This method facilitates the investigation of time-dependent effects due to transient F-actin crosslinking. The elastic component of bundle response is characterized using the homogeneous rod model and results are discussed in the context of cell mechanics. Our measurements show a wide variety of relaxational behaviors for reconstituted actin bundles ranging from a purely elastic response for short deformation times to an elasto-plastic response at long times.

Materials and methods

Protein preparation, bead functionalization, and bundle formation

G-actin and myosin II were prepared from rabbit muscle as previously described in Smith et al. (2007). Monomeric actin was polymerized by addition of F-buffer (0.1 M KCl, 1 mM $MgCl_2$, 0.1 mM $CaCl_2$, 0.5 mM Tris HCl pH 7.8) at a concentration of 5 μM in the presence of rhodamine-phalloidin (Sigma-Aldrich, St. Louis, MO, USA). Myosin II was treated with n-ethylmaleimide (NEM) to deactivate motor function while leaving the molecule structurally intact and able to bind irreversibly to F-actin (Meeusen and Cande 1979; Sheetz et al. 1984). NEM-myosin II was stored for up to one month on ice in a high salt (HiS) buffer (500 mM KCl, 4 mM $MgCl_2$, 20 mM K Phosphate, 1 mM EGTA, pH 7.2).

Polystyrene beads (Polysciences Europe GmbH, Eppelheim, Germany) of 2 and 6 μm were functionalized by overnight incubation with NEM-myosin II at 4°C to facilitate attachment of the protein to the bead surface. Beads were then washed again one or two times by sedimentation and supernatant replacement using HiS. The beads were used for up to 3 days.

For depletion force induced (DFI) bundle experiments, rhodamine-phalloidin actin was diluted in F-buffer containing 0.8% methyl cellulose (MC) as bundling agent, glucose/glucose oxidase as anti-bleaching agent and beads to a final concentration of 50 nM. For α-actinin bundle experiments, 0.1 μM rhodamine-phalloidin actin was pre-bundled in F-buffer containing 0.6% MC, after which 0.1 μM α-actinin (Tebu-Bio, Offenbach, Germany) was added. The pre-bundling step was necessary in order to obtain individual bundles that are not interconnected. Several reports (Lai et al. 2007; Fazli and Golestanian 2007) suggest that it also poses an upper limit to the the bundle size of ~30 filaments. In fact, by comparing fluorescence intensity of DFI-bundles to single filaments we obtained bundle sizes of 20–70 filaments. This solution of F-actin bundles was then further diluted 3.3× using anti-bleach F-buffer containing additional α-actinin and beads to final actin and α-actinin concentrations of 30 and 50nM, respectively. Using rate constants from Wachsstock et al. (1993) this provides for approximately one out of 13 monomers being bound to a crosslinker in chemical equilibrium. Although samples were incubated for 30–60 min, at least two to four times longer than needed for plastic deformation to occur, allowing for crosslinkers to diffuse into the bundle, it is beyond experimental control how homogenous α-actinin is eventually distributed. It was verified that the final MC content of 0.18% was below the bundling threshold.

About 7–10 μl of the final solution were deposited on a Sigmacote-treated (Sigma-Aldrich) 22 mm × 22 mm coverslip with vacuum grease-lined edges. A 24 mm × 50 mm coverslip was placed on top of the drop and then pressed flat, with care taken to remove trapped air pockets. The sample chamber was pressed together between two aluminum plates in a controlled fashion with a micrometer screw. The larger beads were immobilized between the two coverslips and used to control the approximate sample thickness. For deformation experiments, large beads with attached bundles were located and freely floating smaller beads could then be optically trapped and subsequently attached to the bundles' free ends.

Two approaches to verify bundle size in situ were considered but proved to be infeasible. First, comparing fluorescence intensity of bundles to filaments failed for lack of identifiable single filaments in the vicinity of the bundle under consideration. The second approach involved analysis of thermal motion of the bundles prior to deformation experiments. However, it was impossible to collect a statistically significant number of fluorescence images without jeopardizing the central experiment due to photobleaching.

Optical tweezers and fluorescence detection

The optical tweezers used in the experiments have been previously described in Koch et al. (2004), Stuhrmann et al. (2006). A Hamamatsu Orca ER digital CCD camera (Hamamatsu Photonics Deutschland GmbH, Herrsching am Ammersee, Germany) was used to observe samples and record fluorescence microscopy images.

For data acquisition, all components were controlled and integrated by a self-written LabVIEW (National Instruments, Munich, Germany) program that allowed visualization of fluorescent beads and rhodamine-phalloidin labeled F-actin. Fluorescence images of beads and bundles were recorded and bead positions were determined later by cross-correlation analysis.

Experimental procedure

Two types of bundles were used in the deformation experiments. The first type was formed by α-actinin. In the second case only depletion forces without additional protein crosslinks formed so-called DFI bundles (Hosek and Tang 2004). The depletion force method was used for both types of bundles because it consistently produced individual, long, thick, and relatively well-formed bundles.

F-actin bundles were bent into curved configurations by trapping a 2 μm bead in the optical tweezers and connecting it to a bundle attached to an immobilized 6 μm bead. The bundle was then deformed by the angle θ as shown in Fig. 1. To standardize the extent of deformation, the mean radius of curvature of the bundle was approximated based on its length and the deformation angle given. Assuming the bundle contour to be a segment of a circle with radius R, the radius of curvature is determined by $R = \frac{L}{2\theta}$. A maximum radius of curvature in the range of 2–5 μm was found to be optimal in producing significant bending without breaking or damaging the bundles.

Moving the bundle in a purely circular arc was found to stretch the bundles and force them to act as stiff levers, concentrating considerable strain at the contact points with the larger beads due to the clamped boundary conditions. To avoid damaging the bundle near the attachment sites, the distance of the attachment point to the trapped bead was decreased by a factor of $\frac{1}{\theta}\sin(\theta)$ in successive steps while bending. This factor was chosen such that attachment point and bead limit a circular segment tangential in the attachment point of the length of the bundle.

After reaching the maximum deformation angle θ_0, the bead was held for short or long holding times and subsequently released, allowing the bundle to relax freely in solution. Fluorescence images of both the trapped bead and the bundle were recorded before, during (holding times $\leq$10 s), and after the deformation. Upon release the relaxation behavior of F-actin bundles was characterized by plotting the trajectories of the attached 2 μm beads over time. The bead trajectory was parameterized in terms of the bending angle θ (Fig. 1), starting with the maximum angular displacement θ_0 and relaxing towards the undeformed bundle configuration, $\theta = 0$.

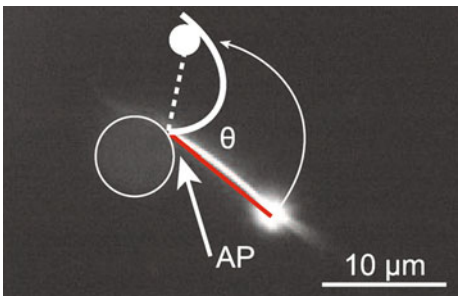

Fig. 1 Large deformation of F-actin bundles using optical tweezers. Upon attachment of the smaller bead to the bundle near its free end, the attachment point of the bundle to the larger bead (labeled AP) and the center of the smaller, optically trapped bead are determined manually. Using this input the control program then determines the nominal bundle contour (*red line*). A deformation angle, θ, between the bundle contour and the putative final position of the bead (*dotted line*) is chosen. The bundle is bent by movement of the bead along a subcircular arc (See "Materials and methods") to a position corresponding to the deformation angle, as depicted by a *curved arrow*. A hypothetical bent bundle is shown to illustrate the outcome

The reproducibility of elastic bundle response after large deformations was probed by repeated bending with short holding times. α-actinin bundles were bent multiple times in opposite directions (Fig. 2a). In this experiment, the bundle was bent first in one direction 5 times using 5 s holding time each, and subsequently bent in the opposite direction using the same procedure. The bundle relaxed fully after each of these bends, demonstrating that the measurement of elastic response is reproducible. DFI bundles were subjected to similar repeated bends (Fig. 2b), although longer relaxation times prevented deformation in two directions because of photobleaching. DFI bundles also fully relaxed; these experiments demonstrate that the elastic response to short timescale deformations is reproducible and that this method effectively and robustly probes the relaxation behavior without noticeably damaging the bundles.

Results

Large bending deformations of F-actin bundles

In order to overcome the limit in extent of deformation due to passive, thermal fluctuations, F-actin bundles were attached to two beads, one of which had been fixed to the

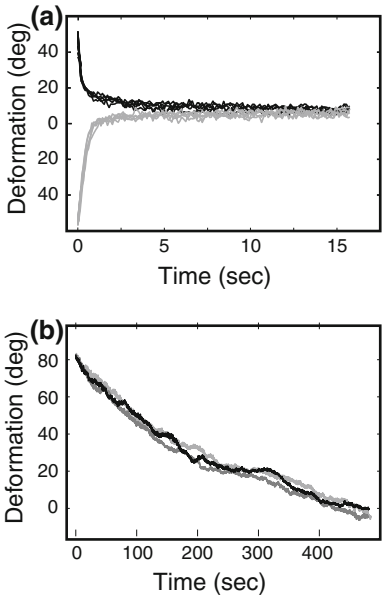

Fig. 2 Relaxation behavior of F-actin bundles deformed repeatedly using short holding times. **a** DFI-α-actinin bundle bent five times in one direction and then five times in the opposite direction with a holding time of 5 s each time. **b** DFI bundle bent three times in one direction and held for 10 s each time. Both experiments show that the response is reproducible, suggesting that bundles are not significantly damaged by the deformations

substrate. The second bead was trapped by optical tweezers and used to bend the bundle into a curved configuration (Fig. 1).

When repeatedly bending a bundle, the times for it to recover its undeformed state varied by a factor of two to three. However, comparing all bundles we probed, relaxation times adjusted for bundle length show a spread over almost two orders of magnitude (Fig. 3).

Time-dependent bundle mechanical response to large deformation

To probe the time-dependent mechanical response of α-actinin crosslinked F-actin bundles, bundles were subjected to repeated large deformations using short (5 s) and long (1,000 s) holding times (Fig. 4a, b). Two orders of magnitude differences in holding time were chosen to illustrate clear differences in bundle response (see also Online Resource Fig. S1). In all experiments the position of the bead was used to monitor bundle deformation. After the first short holding time bend in Fig. 4a, the bundle fully relaxed in approximately 60 s. This is in contrast to the subsequent long holding time bend, in which the bundle exhibited only partial relaxation in approximately 80 s. This bundle did not relax further, even after tens of minutes. Although these two time constants are comparable for the same bundle, those of other bundles differ significantly.

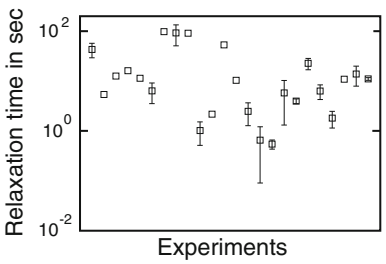

Fig. 3 Relaxation time constants for 24 different alpha-actinin crosslinked F-actin bundles. *Error bars* designate standard deviation if more than one measurement with a holding time of 5 to 10 s was performed per bundle

Next, the deformation-relaxation process was repeated using a short holding time, but the optically trapped bead was moved to the original, undeformed position (Fig. 4c) after which the bundle exhibited nearly full return to its new resting position (yellow circle) in approximately 140 s. In this experiment, dubbed the "integrity test", the bundle nearly fully returned to its new resting position, demonstrating that the bundle was not damaged in the first combination of short and long holding-time bends. Often a second long holding-time bend to the original, undeformed position could be applied after which no relaxation was observed. This experiment demonstrates that plastic bundle deformation is fully reproducible, and thus independent of the previous history of bundle deformation. Relaxation trajectories from the first two deformations of the bundle corresponding to Fig. 4a, b exhibited exponential decay, suggesting a single physical process governing the relaxation response.

The existence of full and partial bundle relaxation behaviors suggests that crosslinked F-actin bundles exhibit both elastic and plastic mechanical response depending on loading time or rate. This effect was found consistently for α-actinin bundles, observed in a total of ten different bundles. To quantify the time-dependent relaxation behavior, the residual deformation was determined for each complete set of bending experiments (Fig. 5). It was defined as the ratio between the long-time relaxation plateau values, θ_∞, and the initial deformation angles, θ_0. Plateau values, θ_∞, represent the average final resting configurations of the bundles, showing the extent of relaxation for a particular deformation.

Short holding times (5–10 s) resulted in a full return to the undeformed state, whereas long holding times (1,000 s) resulted in only partial return to the undeformed configuration, consistently exhibiting significant residual deformation. In addition, "integrity" tests demonstrate reproducibility of this behavior, indicating that bundles are not damaged irreversibly during plastic deformation.

In order to probe the molecular origin of the observed plastic deformation, deformation experiments were performed on F-actin bundles formed without internal protein

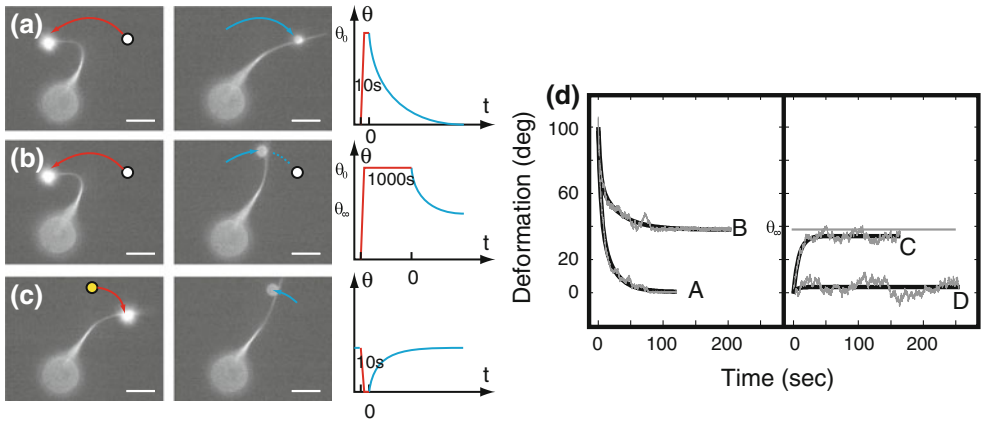

Fig. 4 Experimental probe of time-dependent F-actin bundle relaxation behavior following large deformations using optical tweezers. See also Online Resources movies M1, M2 and M3. **a** (M1) Short hold bend. The F-actin bundle is bent to the bending angle θ_0 by optical tweezers and held there for 10 s (*red*). Full relaxation occurs in approximately 60 s after the bead's release (*cyan*). **b** (M2) Long hold bend. The same bundle as in A is deformed again to θ_0 but using a 1,000 s hold (*red*). Partial return of the bundle to its new resting position θ_∞ occurs in approximately 80 s (*cyan*). The ratio $\frac{\theta_\infty}{\theta_0}$ is termed residual deformation (Fig. 5). **c** (M3) Integrity test bend. The bundle is forcibly returned to its original undeformed position, $\theta = 0$, and held there for 10 s (*red*). It then returns to its newly acquired resting position (*yellow circle*) in approximately 140 s (*cyan*), showing that it is not damaged in the first combination of short and long holding-time bends. *Scale bar* 5 μm. **d** Relaxation trajectories of a bead are used to parameterize bundle relaxation. *Graphs A* and *B* refer to short and long holding-time bends as in *panels a* and *b* showing full and partial relaxation. After the integrity test shown by *graph C* as in *panel c*, the bundle is held for 1,000 s at the original undeformed position, $\theta = 0$. After release the bundle fluctuates around this position, *graph D*

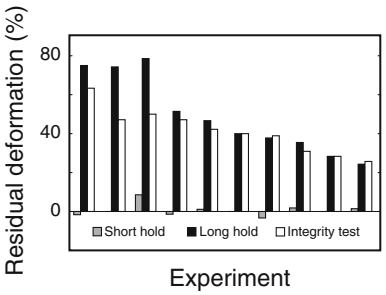

Fig. 5 Characterization of F-actin bundle plasticity in terms of residual deformation $\frac{\theta_\infty}{\theta_0}$. Short holding times (5–10 s) result in little or no residual deformation, whereas long holding times (1,000 s) show a significant percentage, illustrating the difference in the two responses. Integrity test deformations with short holding times result in a return of the bundles to their new resting configurations. Each group of bars corresponds to one experiment

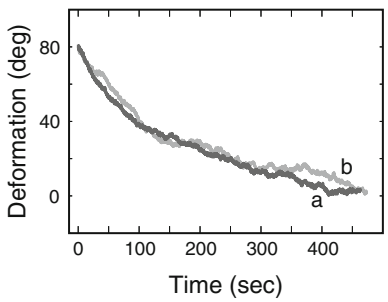

Fig. 6 Relaxation of DFI bundles after large deformations. DFI bundles were deformed for 10 s (**a**) and 1,000 s (**b**) holding times, showing no evidence of plasticity in either case

crosslinks via depletion-forces (DFI bundles). In contrast to α-actinin bundles, these DFI bundles did not exhibit plasticity either for short or for long holding times (Fig. 6). Instead, large deformations of these bundles consistently resulted in full return to the original bundle configurations without any evidence of plasticity, or residual deformation. Relaxation times were longer than those of α-actinin bundles which can be fully attributed to the 15 × higher solution viscosity that contributes to the relaxation time via the drag coefficient in a linear fashion (Eq. 1). The absence of a plastic regime for DFI bundles suggests that these bundles do not contain internal dissipative mechanisms as present in α-actinin crosslinked bundles.

Characterization of bundle relaxation

A natural first approach to characterizing the temporal relaxation behavior of the bundles is to determine the characteristic time scale of the process using an exponential fit to the bead trajectory. Assuming the bundle to be a homogeneous elastic rod, bending modes relax exponentially with τ_n

$$\tau_n = \frac{\zeta L^4}{\kappa q_n^4}, \tag{1}$$

where ζ is the drag coefficient per unit length, L is the length of the bundle, and κ is its bending stiffness (Aragon and Pecora 1985). $q_n = (n - \frac{1}{2})\pi$ gives the mode dependence for the boundary conditions of one free and one

clamped end (Taute et al. 2008) separating τ_1 and τ_2 for the lowest and second mode, respectively, by a factor of 80. At 10 fps and decay times of at most 100 s higher modes cannot be reliably resolved.

The relaxation response of many α-actinin bundles is fit well by a single exponential, as demonstrated by residual analysis (Fig. 7a). Characteristic times of elastic and partially plastic relaxations of the same bundle differ by no more than a factor of two to three. In order to compare different bundles, the ratio $\frac{\tau_1}{L^4}$ is calculated to normalize for bundle length, since the thickness of the bundle and thus its drag coefficient are experimentally inaccessible. Values for all bundles span almost two orders of magnitude, despite adhering to a common bundle preparation protocol.

In some cases, however, bead trajectories are not well fit by a single exponential (Fig. 7b). Instead, a double exponential is fit to these trajectories and the residuals of both fits are compared. In cases where the double exponential fit is more appropriate, the two relaxation time constants typically differ by a factor of 10 to 40. Visual inspection of the bundle backbone suggests that the double exponential relaxation behavior is associated with a strongly non-uniform strain distribution along the bundle, manifested as a local "kink" intervening between two relatively straight bundle sections (Fig. 8). The initial fast relaxation observed here is likely due to an initial straightening of the kink followed by a slower relaxation process.

Discussion

Large deformations of F-actin bundles crosslinked by α-actinin show at least two relaxation behaviors depending on the length of time that the bundle is held in the maximally deformed configuration before being released: for short holding times, bundles exhibit elastic response, fully returning to their initial configuration (Fig. 4a), whereas for long holding times, bundles exhibit plastic deformation, evident in residual deformation that does not relax on the time scales observed (Figs. 4b, 5). α-actinin is a crosslinking protein that is present in cytoskeletal structures such as stress fibers and the contractile ring, often together with myosin II, suggesting a possible physiological role for the differential elasto-plastic response of these bundles: On short time scales these cellular processes retain a "memory" of their initial state, whereas on longer time scales they adopt their new, deformed configuration as their

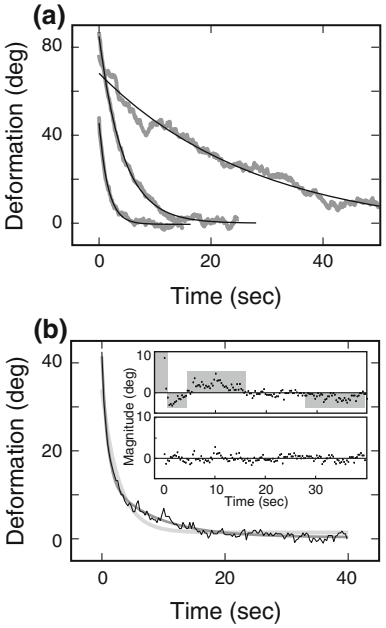

Fig. 7 Fits to the relaxation bead trajectories of the first deformation after a short holding time. **a** Three examples of single exponential fits (*black*) to the data (*gray*). The corresponding time constants are 1.6, 4.2 and 21 s, with coefficients of determination, R^2, 0.96, 0.96 and 0.97, respectively. **b** Single (*light gray line*, $R^2 = 0.92$), and double (*dark gray line*, $R^2 = 0.98$) exponential fits. (*Inset*) Residuals for both single (*upper*) and double (*lower*) exponential fits showing that the double fit is more appropriate. *Gray boxes* in the single exponential plot highlight areas indicating that the actual bundle is relaxing faster, slower and faster again than described by the fit function

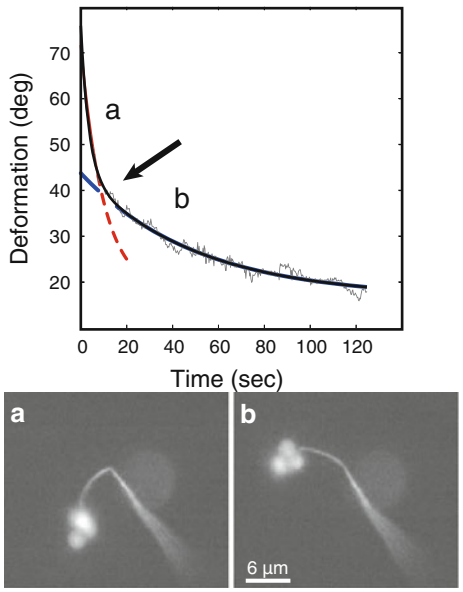

Fig. 8 Relaxation behavior of a strongly kinked bundle showing two separate relaxation regimes. (See also M4) (*Upper*) Graph of the relaxation trajectory characterized by a double exponential fit (*black line*). *Red* and *blue lines* show the two single exponentials that comprise the double exponential and demarcate different bending regimes. In regime (**a**), the bundle relaxes rapidly for the first 8 s with a characteristic relaxation time of $\tau = 6.4$ s. After the crossover region (*black arrow*), the relaxation in regime (**b**) is characterized by a second exponential with $\tau = 220$ s. (*Lower*) Fluorescence images of the bundle after release from the trap corresponding to regimes *a* and *b* above. a was taken immediately after release of the bead and b was taken 40 s later

ground-state. Such differential mechanical response might be essential to facilitating cytoskeletal rearrangements during wound healing, cellular division, and motility.

By reproducing both elastic and plastic deformation on previously deformed bundles, the permanent, plastic mechanical response of F-actin bundles is demonstrated to be due to the internal rearrangement of filament-connecting crosslinking proteins and not to damage to filaments themselves. In some cases, a third plastic deformation of the bundle following the integrity test was also possible. Further evidence that crosslink rearrangement is responsible for plastic deformation of F-actin bundles is provided by bundles formed using depletion forces alone. These bundles exhibited purely elastic response even after long holding times of 1,000 s (Fig. 3), without any evidence of permanent, plastic deformation. Taken together, these data suggest that plastic bundle deformation is due to the presence of the dynamic crosslinking protein α-actinin, which undergoes continuous association and dissociation with actin filaments, stabilized here using rhodamine-phalloidin. These stochastic crosslink binding-unbinding events allow internal crosslinks that have been sheared by filaments sliding with respect to each other to reorganize during long holding times, resulting in a stable new resting configuration of the bundle that retains its bent configuration.

Long holding times of 1,000 s were required here to differentiate clearly between purely elastic and elasto-plastic F-actin bundle response (for intermediate holding times see supplemental Figure S1). This holding time was considerably longer than the time required for unbinding and rebinding of individual α-actinin molecules inferred from association rates of approximately 1–4 $\mu M^{-1}s^{-1}$ and dissociation rates of approximately 0.1–0.4 s^{-1} measured in bulk (Xu et al. 1998). F-actin networks crosslinked with α-actinin have been shown to reorganize in tens of seconds (Wachsstock et al. 1993). There are several possible explanations for the long holding time required to exhibit a differential elasto-plastic response in F-actin bundle bending. First, the dense structure of F-actin bundles may somewhat limit crosslinker diffusion within the bundle. Second, the effective rate of association of crosslinks may be reduced considerably due to the helical geometry of the actin filament that limits the number of available adjacent binding sites to crosslink neighboring filaments. In contrast to bulk networks, crosslinking proteins and filaments may thus be effectively trapped near their current position. Further investigation will be required to resolve the precise molecular origin of the long holding times required to exhibit plastic bundle response.

The homogeneous elastic rod model adequately describes the elastic response of many of the F-actin bundles examined. However, numerous cases of α-actinin-crosslinked bundles were found in which a single exponential fit was insufficient to describe the elastic response. There are a number of potential causes of the deviation from the relaxation behavior of a simple rod, including the possibility of inhomogeneities in bundle structure that might allow multiple relaxation processes to occur (Fig. 8). In theoretical considerations, filament size is typically considered to span the full length of the bundle (Bathe et al. 2008). In reality, filament fractures are geometric discontinuities that may provide defects that result in deformations with distinct relaxation behaviors.

To differentiate between distinct contributions to relaxation behavior that are not characterized by a single exponential, further experiments are needed to probe relaxation mechanisms in a frequency or bending mode dependent manner. In addition, systematic investigation of deformation magnitudes and holding times could provide further insight into the dynamic and mechanical behavior of crosslinked F-actin bundles. However, the present study already points towards a variety of mechanisms that influence bundle response to deformation, which are possibly beyond experimental control.

Even considering the strong dependence of relaxation times on the length of the bundle, elastic responses of different bundles span almost two orders of magnitude. The bending stiffness κ and thus the inverse of the characteristic relaxation time τ_1 scales with the number of filaments or its square and consequently with the square or fourth power of the bundle diameter, depending on the type of crosslinking (Bathe et al. 2008). The uncertainty in bundle size of 20–70 filaments would account for the approximately one order of magnitude spread observed. Additionally, it is ambiguous whether α-actinin is able to penetrate the compact preformed actin bundle ("Materials and methods") and separate filaments by its preferred interfilament distance of 40 nm (Lai et al. 2007) giving rise to another 25% spread in drag coefficient ζ and consequently in relaxation time τ_1.

Similar to the heterogeneity in bundle constitution, morphology, and mechanics observed here, stress fibers in adherent cells are also highly heterogeneous in their morphology (Katoh et al. 1998) and mechanical properties varying even locally within stress fibers (Kumar et al. 2006). It could be of theoretical interest to understand to what extent the resulting broad spectrum of relaxation times might contribute to the observed scale-free rheological behavior of cells (Fabry et al. 2001; Fernandez et al. 2006; Trepat et al. 2008; Semmrich et al. 2007), potentially pointing towards the molecular origin of such a scaling behavior. This is supported by the observation that adherent cells, which display a large number of stress fibers, show the multirelaxation behavior described above, while suspended cells, in which stress fibers are absent, show a well defined terminal relaxation time (Wottawah et al. 2005).

Notwithstanding, the present study highlights the important role that dynamic crosslinks play in conferring differential elasto-plastic response to F-actin bundles. In living cells, dynamic crosslinking is needed for stress fibers to rearrange in response to external mechanical and chemical cues, potentially allowing for cellular "memory" of original, undeformed states that is slowly dissipated with time as cells reorganize to stabilize new configurations. Further investigation of the elasto-plastic behavior of F-actin bundles is likely to reveal novel physiological roles for these ubiquitous cytoskeletal structures.

Acknowledgments We thank Florian Huber, Jens Glaser and Klaus Kroy for helpful discussions. This work was supported by Leipzig School of Natural Sciences, "Building with Molecules and Nano-Objects" (BuildMoNa), and by DFG Graduiertenkolleg "InterNeuro" (GRK 1097) in Leipzig. M.B. is supported by MIT faculty start-up funds and the Samuel A. Goldblith Career Development Professorship. C.H. was supported by the Humboldt Foundation in the form of a Feodor Lynen research fellowship.

References

Aragon SR, Pecora R (1985) Dynamics of wormlike chains. Macromolecules 18(10):1868–1875. doi:10.1021/ma00152a014

Aratyn YS, Schaus TE, Taylor EW, Borisy GG (2007) Intrinsic dynamic behavior of fascin in filopodia. Mol Biol Cell 18(10):3928–3940. doi:10.1091/mbc.E07-04-0346

Bartles JR (2000) Parallel actin bundles and their multiple actin-bundling proteins. Curr Opin Cell Biol 12(1):72–78. doi:10.1016/S0955-0674(99)00059-9

Bathe M, Heussinger C, Claessens MM, Bausch AR, Frey E (2008) Cytoskeletal bundle mechanics. Biophys J 94(8):2955–2964. doi:10.1529/biophysj.107.119743

Claessens MMAE, Bathe M, Frey E, Bausch AR (2006) Actin-binding proteins sensitively mediate F-actin bundle stiffness. Nat Mat 5(9):748–753. doi:10.1038/nmat1718

Fabry B, Maksym GN, Butler JP, Glogauer M, Navajas D, Fredberg JJ (2001) Scaling the microrheology of living cells. Phys Rev Lett 87(14):148–102. doi:10.1103/PhysRevLett.87.148102

Fazli H, Golestanian R (2007) Aggregation kinetics of stiff polyelectrolytes in the presence of multivalent salt. Phys Rev E 76(4):041–801.doi:10.1103/PhysRevE.76.041801

Fernandez P, Pullarkat PA, Ott A (2006) A master relation defines the nonlinear viscoelasticity of single fibroblasts. Biophys J 90(10):3796–3805. doi:10.1529/biophysj.105.072215

Ferrer JM, Lee H, Chen J, Pelz B, Nakamura F, Kamm RD, Lang MJ (2008) Measuring molecular rupture forces between single actin filaments and actin-binding proteins. Proc Natl Acad Sci USA 105(27):9221–9226. doi:10.1073/pnas.0706124105

Heintzelman MB, Mooseker MS (1992) Assembly of the intestinal brush border cytoskeleton. Curr Top Dev Biol 26:93–122

Heussinger C, Schaefer B, Frey E (2007) Nonaffine rubber elasticity for stiff polymer networks. Phys Rev E Stat Nonlin Soft Matter Phys 76(3 Pt 1):031,906

Hoffman BD, Massiera G, Citters KMV, Crocker JC (2006) The consensus mechanics of cultured mammalian cells. Proc Natl Acad Sci 103(27):10259–10264. doi:10.1073/pnas.0510348103

Hosek M, Tang JX (2004) Polymer-induced bundling of f actin and the depletion force. Phys Rev E 69(5):051,907. doi:10.1103/PhysRevE.69.051907

Hotulainen P, Lappalainen P (2006) Stress fibers are generated by two distinct actin assembly mechanisms in motile cells. J Cell Biol 173(3):383–394. doi:10.1083/jcb.200511093

Howard J (2001) Mechanics of Motor Proteins and the Cytoskeleton. Sinauer Associates, Inc., Sunderland

Janmey PA, Hvidt S, Käs J, Lerche D, Maggs A, Sackmann E, Schliwa M, Stossel TP (1994) The mechanical properties of actin gels. elastic modulus and filament motions. J Biol Chem 269(51):32503–32513

Käs J, Strey H, Tang JX, Finger D, Ezzell R, Sackmann E, Janmey PA (1996) F-actin, a model polymer for semiflexible chains in dilute, semidilute, and liquid crystalline solutions. Biophys J 70(2)

Katoh K, Kano Y, Masuda M, Onishi H, Fujiwara K (1998) Isolation and contraction of the stress fiber. Mol Biol Cell 9(7):1919–1938

Koch D, Betz T, Ehrlicher A, Gogler M, Stuhrmann B, Käs J, Dholakia K, Spalding GC (2004) Optical control of neuronal growth. In: Optical Trapping and Optical Micromanipulation, SPIE, Denver, CO, USA, vol 5514, pp 428–436

Koenderink GH, Dogic Z, Nakamura F, Bendix PM, MacKintosh FC, Hartwig JH, Stossel TP, Weitz DA (2009) An active biopolymer network controlled by molecular motors. Proc Natl Acad Sci 106(36):15192–15197. doi:10.1073/pnas.0903974106

Kumar S, Maxwell IZ, Heisterkamp A, Polte TR, Lele TP, Salanga M, Mazur E, Ingber DE (2006) Viscoelastic retraction of single living stress fibers and its impact on cell shape, cytoskeletal organization, and extracellular matrix mechanics. Biophys J 90(10):3762–3773. doi:10.1529/biophysj.105.071506

Lai GH, Coridan R, Zribi OV, Golestanian R, Wong GCL (2007) Evolution of growth modes for polyelectrolyte bundles. Phys Rev Lett 98(18):187,802. doi:10.1103/PhysRevLett.98.187802

Meeusen RL, Cande WZ (1979) N-ethylmaleimide-modified heavy meromyosin. a probe for actomyosin interactions. J Cell Biol 82(1):57–65

Pollard T, Earnshaw W (2002) Cell biology. Elsevier Science, Philadelphia

Ridley AJ, Schwartz MA, Burridge K, Firtel RA, Ginsberg MH, Borisy G, Parsons JT, Horwitz AR (2003) Cell migration: integrating signals from front to back. Science 302(5651):1704–1709. doi:10.1126/science.1092053

Roberts WM, Howard J, Hudspeth AJ (1988) Hair cells: transduction, tuning, and transmission in the inner ear. Ann Rev Cell Biol 4:63–92. doi:10.1146/annurev.cb.04.110188.000431

Semmrich C, Storz T, Glaser J, Merkel R, Bausch AR, Kroy K (2007) Glass transition and rheological redundancy in f-actin solutions. Proc Natl Acad Sci 104(51):20199–20203. doi:10.1073/pnas.0705513104

Sheetz M, Chasan R, Spudich J (1984) ATP-dependent movement of myosin in vitro: characterization of a quantitative assay. J Cell Biol 99(5):1867–1871

Shin JH, Mahadevan L, So P, Matsudaira P (2004) Bending stiffness of a crystalline actin bundle. J Mol Biol 337(2):255–261. doi:10.1016/j.jmb.2004.01.028

Smith D, Ziebert F, Humphrey D, Duggan C, Steinbeck M, Zimmermann W, Käs J (2007) Molecular motor-induced instabilities and cross linkers determine biopolymer organization. Biophys J 93(12):4445–4452. doi:10.1529/biophysj.106.095919

Stuhrmann B, Jahnke H, Schmidt M, Jähn K, Betz T, Müller K, Rothermel A, Käs J, Robitzki AA (2006) Versatile optical manipulation system for inspection, laser processing, and isolation of individual living cells. Rev Sci Instrum 77(6):063116-1–063116-11. doi:10.1063/1.2214961

Taute KM, Pampaloni F, Frey E, Florin E (2008) Microtubule dynamics depart from the wormlike chain model. Phys Rev Lett 100(2):028102-1–028102-4. doi:10.1103/PhysRevLett.100.028102

Tolomeo JA, Holley MC (1997) Mechanics of microtubule bundles in pillar cells from the inner ear. Biophys J 73(4):2241–2247

Trepat X, Lenormand G, Fredberg JJ (2008) Universality in cell mechanics. Soft Matter 4(9):1750–1759

Wachsstock D, Schwartz W, Pollard T (1993) Affinity of alpha-actinin for actin determines the structure and mechanical properties of actin filament gels. Biophys J 65(1):205–214. doi:10.1016/S0006-3495(93)81059-2

Wottawah F, Schinkinger S, Lincoln B, Ananthakrishnan R, Romeyke M, Guck J, Käs J (2005) Optical rheology of biological cells. Phys Rev Lett 94(9):098–103. doi:10.1103/PhysRevLett.94.098103

Xu J, Wirtz D, Pollard TD (1998) Dynamic cross-linking by alpha-Actinin determines the mechanical properties of actin filament networks. J Biol Chem 273(16):9570–9576. doi:10.1074/jbc.273.16.9570